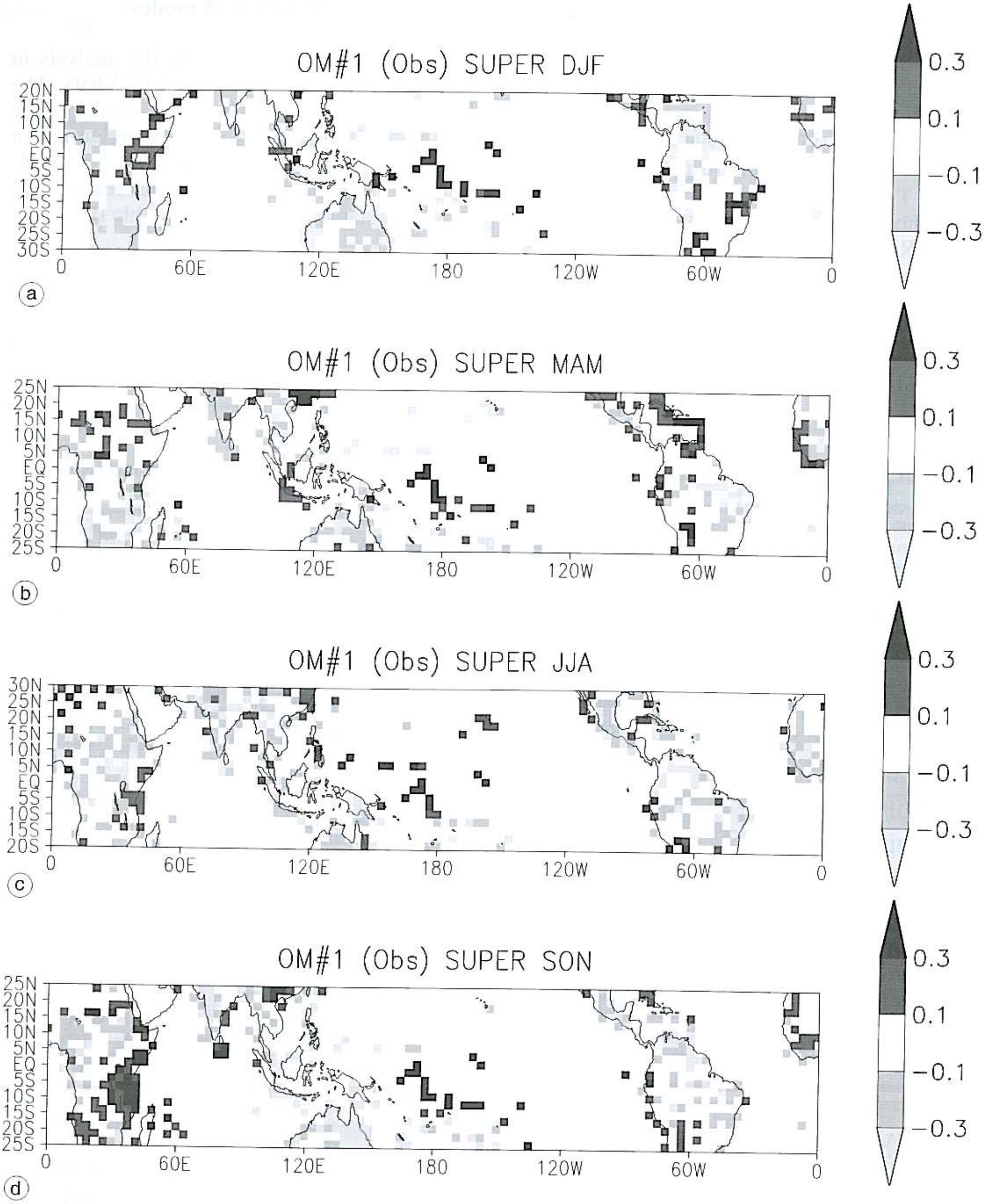


**Fig. 6a-d.** Heterogeneous correlations pattern of super-ensemble $OM_o$ in: a) DJF; b) MAM; c) JJA; d) SON. The values indicate the linear correlation between the observed seasonal rainfall anomalies (from the Hulme data set) and the cross-validated first $OM_m$ score (the mean of the 9 runs is considered).

ble experiment: pattern correlations between the four $OM_o$ modes exceeds 0.98 so only the $OM_o$ pattern of the super-ensemble is displayed (fig.6a). The spatial pattern matches almost perfectly the first observed rainfall mode studied by Dai *et al.* (1997). There is an out-of-phase pattern between the Central Pacific islands and almost the remaining tropical belt, except equatorial East Africa, tropical margins of South and Central America. The weights are also in-phase with the Central Pacific. Note also that the explained variance (see Ward and Navarra, 1997) by the first mode is almost equal between the four SVDAs (8.0 to 8.3%).

There are some differences between the $OM_m$ pattern amongst the three models, reflecting the fact that they each have a different response to ENSO forcing. Pattern correlations between the three models range between 0.49 (EC4-LMD) and 0.60 (EC4-EC3). The super-ensemble is logically strongly correlated (over 0.81) with the three models. The Pacific correlations are almost zonally oriented in EC4 and LMD with an out-of-phase dipole contrasting the equatorial area from the Eastern Indian ocean to the Galapagos archipelago with the subtropical Pacific (fig. 7b,c). There are also negative correlations over the Western Indian Ocean in the EC4 pattern. The EC3 pattern matches better the observed pattern with a zonal out-of-phase dipole between the Western Pacific-Maritime continent and the Central-Oriental Pacific. Other areas are usually out-of-phase with the Central Pacific (*i.e.* below normal rainfall in El Niño years), except for the tropical margins of South and Central America. All models have the wrong sign of anomaly over tropical Africa, relative to the observed pattern with misrepresentation of the well-known in-phase evolution between El Niño and equatorial East Africa, and out-of-phase with Southern Africa (fig. 7a-d). The super-ensemble pattern is dominated by the ones of EC4 and LMD and reflects basically the previously discussed meridional dipole in the tropical Pacific.

Mean skill for the modes is always over 0.8 (except for LMD) and the time-series are, as found in MNWR98, dominated by El Niño - La Niña (hereafter EN - LN) alternations (not shown). Positive (resp. negative) values occur during EN (resp. LN). This can be confirmed by computing the cross-correlations between the cross-validated time expansion coefficients of $OM_o$ and $OM_m$ (the mean of the nine runs) of the super-ensemble analysis with the SST field which served to force the three models. The SST correlation pattern with the $OM_o$ and $OM_m$ coefficients are highly similar for DJF (not shown, but see figure 12 of MNWR98), and reflects mainly the well-known ENSO signature in DJF SST (*i.e.* Moron *et al.*, 1998b).

## 5.2. *MAM*

The $OM_o$ are less consistent amongst the models than in DJF, but pattern correlations are still always higher than 0.84 (between EC4 and LMD) and the correlations with the super-ensemble pattern are over 0.95 (fig. 6b). The super-ensemble spatial pattern has evolved somewhat from the DJF one (pattern correlation = 0.46), indicating some changes in the model's response to ENSO as the annual cycle progresses. The highest positive correlations remain located between the Central Pacific and coastal Ecuador. The negative correlations increase relative to DJF over Nordeste, and negative correlations are also now clear of Cambodia and Malaysia (fig. 6b). Their intensity decreases over tropical Southern Africa. Note also an in-phase behavior between the Central Pacific and Southern China (fig. 6b), already observed by Ropelewski and Halpert (1987, 1996) and Halpert and Ropelewski (1992).

The $OM_m$ patterns for the three models correlate with each other in the range 0.54 to 0.57, while the super-ensemble pattern is always correlated above 0.82 with the three models (fig. 8a-d). The main dipole over the Indo-Pacific basin remains largely meridional for EC4 and LMD, and zonal for EC3, which is more consistent with observations. A new feature of MAM is the strong meridional dipole between the tropical North Atlantic (and Northern South America) and the equatorial Atlantic (and bordering areas of Nordeste and the Gulf of Guinea region). The first area is in-phase with Central Pacific. The positive correlations over the tropical North Atlantic are weak for LMD, and large

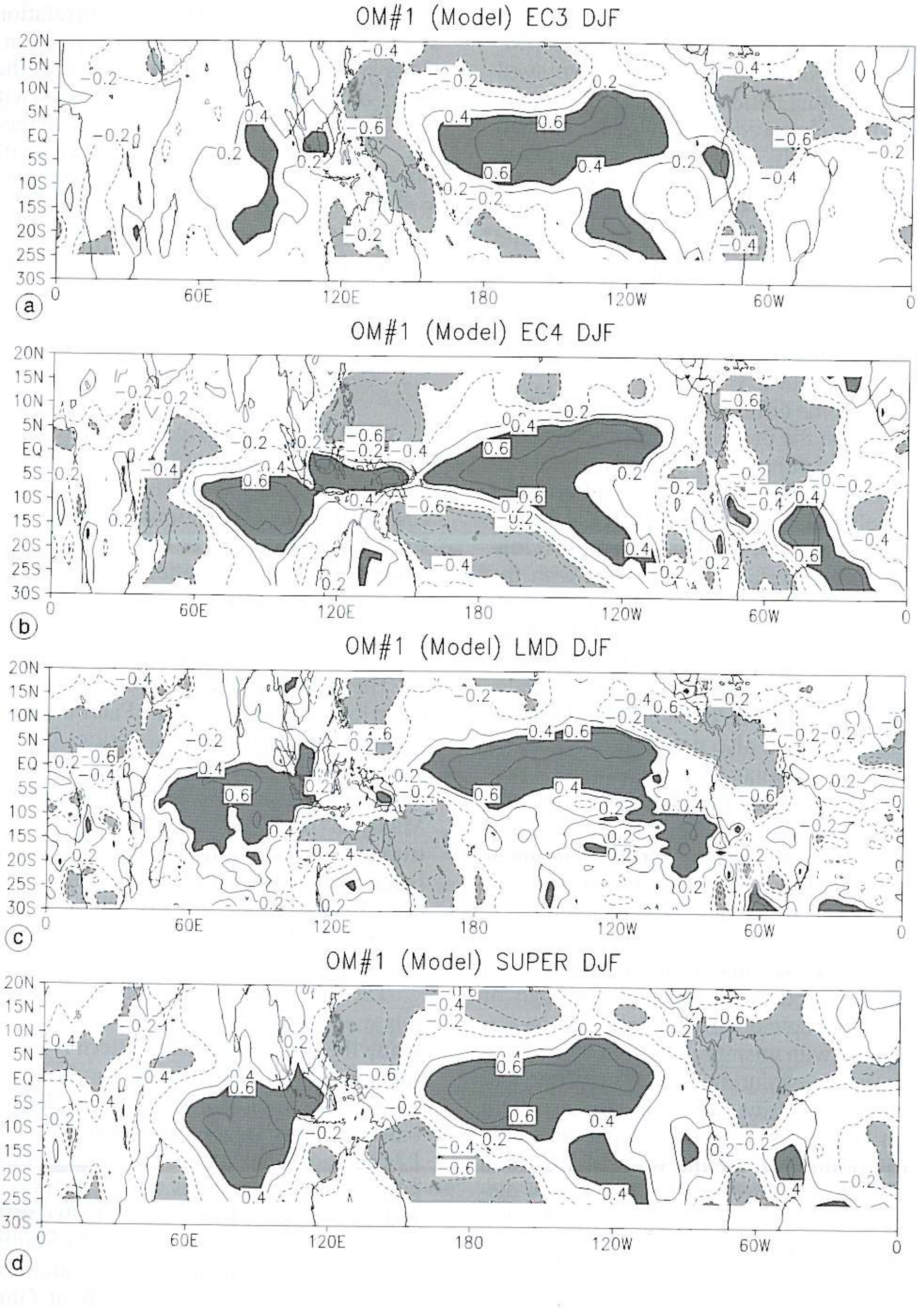


**Fig. 7a-d.** Heterogeneous correlations pattern in DJF for $OM_m$ of: a) EC3; b) EC4; c) LMD; d) super-ensemble. The values indicate the linear correlation between the cross-validated first $OM_o$ score and the simulated mean seasonal rainfall anomalies (from the 3 runs of one model for (a), (b) and (c) and from the 9 runs for (d)).

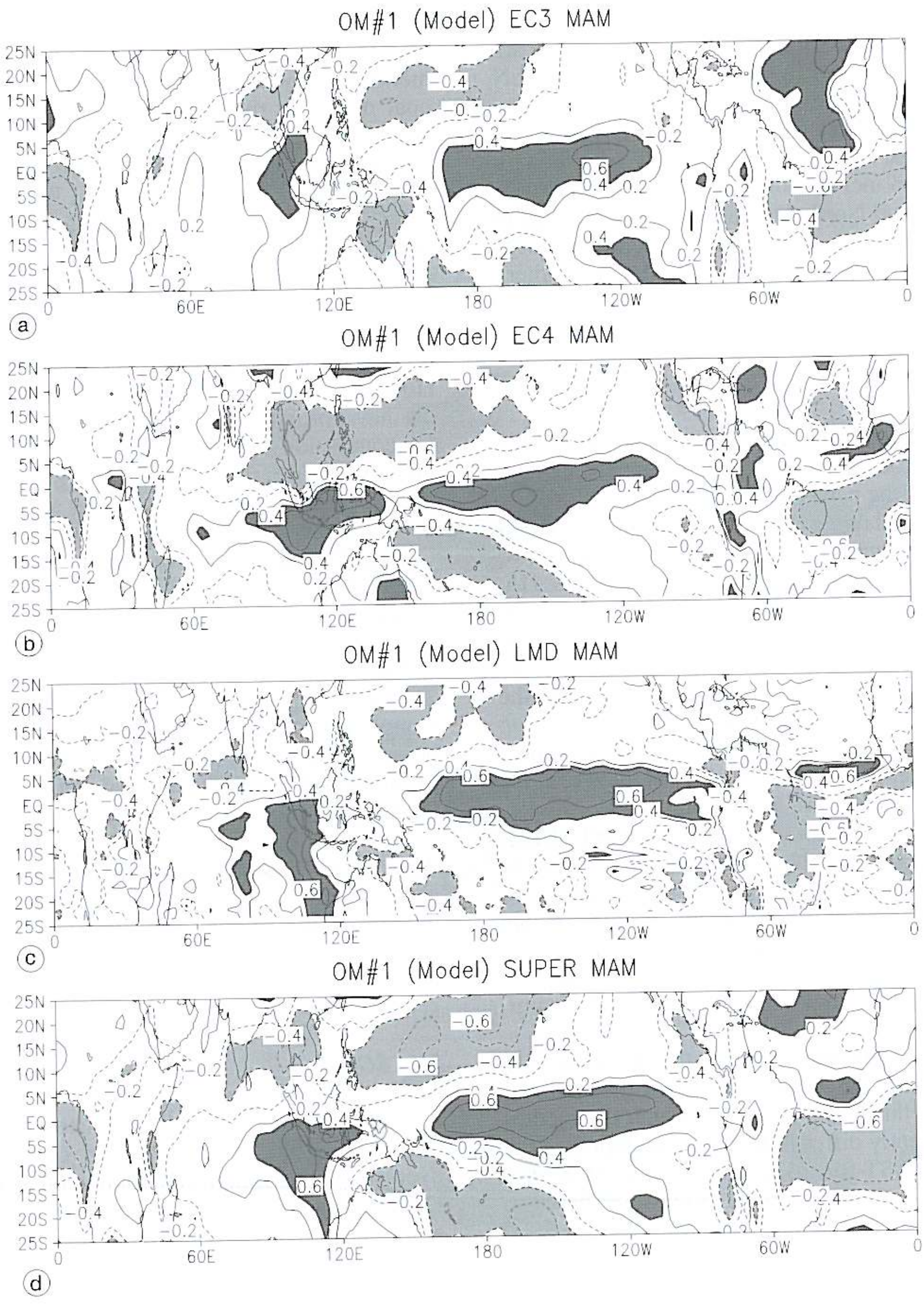


**Fig. 8a-d.** Same as fig. 7a-d except for MAM.

for EC3 (fig. 8a,c). The pattern is weak over the remainder of Africa (fig. 8a-d). Time series are again dominated by alternation of EN and LN (not shown). The correlations between $OM_o$ and $OM_m$ time series and the basic SST field reveal almost the same features as in DJF (not shown), except an increase of positive correlations over the tropical North Atlantic (positively related to equatorial Eastern and Central Pacific) and negative correlations over equatorial and Southern Atlantic.

### 5.3. *JJA*

There are strong changes relative to MAM in the first observed mode, indicating strong evolution in the nature of the leading mode of tropical rainfall (pattern correlations between MAM and JJA super-ensemble $OM_o$ pattern is just 0.35). Amongst the different analyses for JJA, the observed mode changes very little (*e.g.*, pattern correlation is 0.85 between EC3 and LMD and 0.97 between super-ensemble and EC4). The observed mode is almost identical to the pattern already described by Miyakoda *et al.* (1999) and Navarra *et al.* (1999) (fig .6c). There is a clear out-of-phase contrast between the Central and Eastern Pacific plus the Northwestern Pacific around the Philippines and Micronesia on the one hand, and the remaining tropical belt (except Eastern China and Eastern Australia) on the other hand. It implies that when rainfall is anomalously high in the Central and Eastern Pacific, it tends to be anomalously low over the whole domain of the boreal summer monsoon (fig. 6c).

The correlations between the different $OM_m$ patterns are the weakest of all seasons, indicating that this is the season in which the models most greatly differ in their repesentation of the leading SST-forced teleconnection structure: pattern correlations range from 0.38 (between EC3 and LMD) to 0.61 (between EC4 and EC3) and between 0.77 to 0.82 for the correlations between each model and the super-ensemble. There are also some dramatic changes relative to the MAM patterns, with pattern correlations ranging between 0.16 (MAM EC4 *versus* JJA EC4) and 0.47 (MAM EC3 *versus* JJA EC3).

The main change for EC4 and LMD is the gradual transformation (seen in individual monthly analyses, not shown) from the meridional dipole in the Indo-Pacific region during MAM to a zonal one in JJA (fig. 9a-d). LMD exhibits a clear zonal out-of-phase dipole between the New Guinea - Salomon Islands area and the Central and Eastern Pacific (fig. 9a-d), with the Indian peninsula also out of phase with the Central Pacific. This pattern agrees with the observed mode, and indicates that the LMD teleconnection structure response to SST is in accord with observations over these regions. However, over the Atlantic and Africa, all models have problems in capturing the observed teleconnection structure. The EC4 and LMD models are, in particular, both wrong (relative to the observed mode) in developing an in-phase evolution between the Sahelian belt and the Central Pacific. EC3 is somewhat better in this region, but the near-zero weights through the Sahel still suggest a failure to capture the Sahel-ENSO teleconnection. The explained variance and the skill (fig. 9a-d) are lower than in DJF. This season appears to have a strong SST-forced component, but its representation in GCMs appears still to be problematical. The correlation of the modes with SST are very consistent (not shown), again confirming that the different teleconnection structures in the three models all derive from the same SST forcing patterns. The patterns show a strong decrease in correlation over the Indian Ocean (MNWR98). Weak negative correlations now exist over the equatorial Atlantic.

### 5.4. *SON*

The $OM_o$ patterns are very consistent amongst the models, like in DJF (pattern correlations over 0.97). The patterns are more similar to the DJF one (pattern correlation between the super-ensemble $OM_o$ in SON and DJF = 0.41) than the JJA ones (fig. 6a-d). Nonetheless, there are still substantial differences with DJF. For example, the negative correlations over Northern South America are weaker than in DJF. A particular feature of SON (*e.g.*, Ogallo, 1988; Beltrando, 1990; Beltrando and Camberlin, 1993) are the

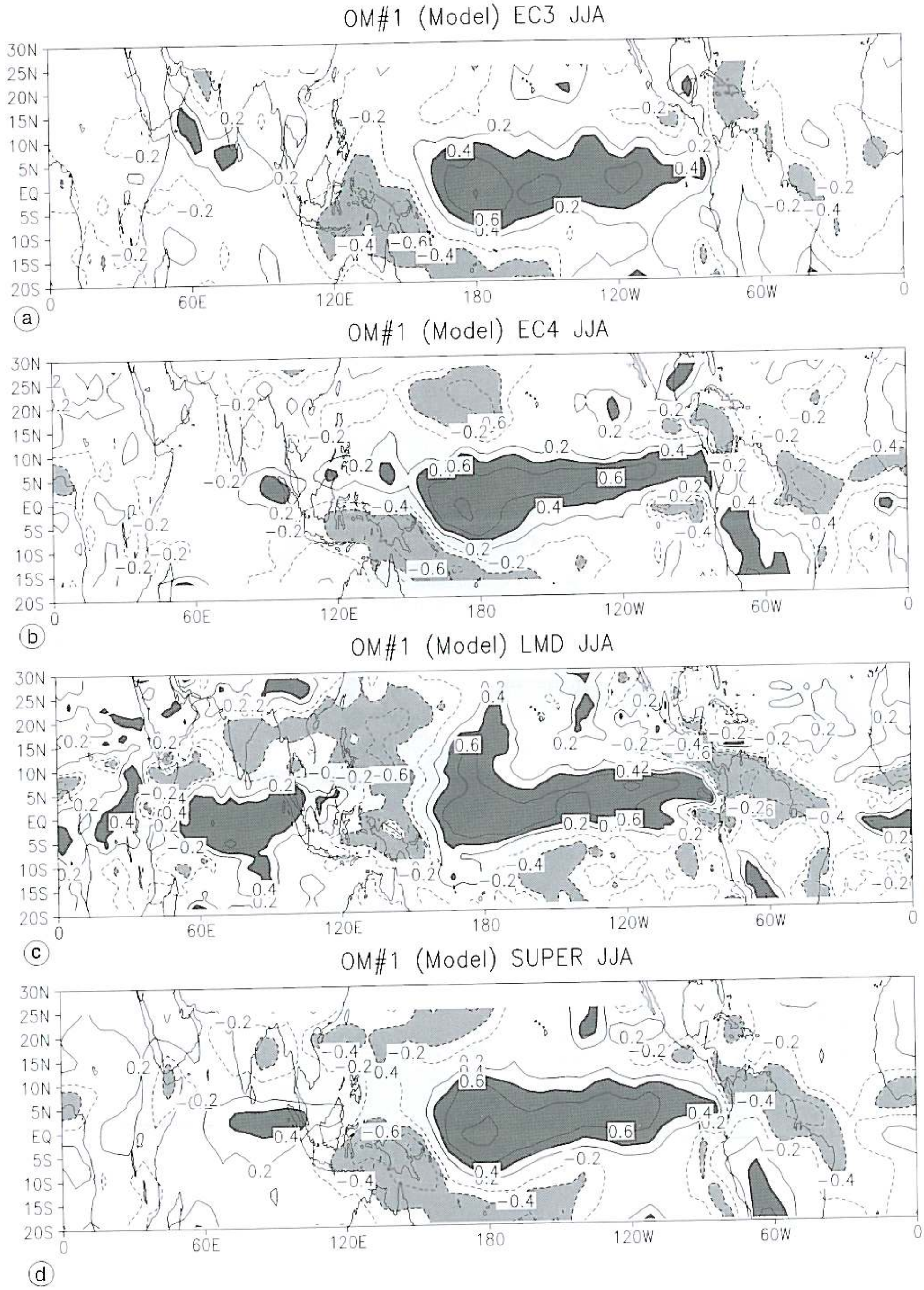


**Fig. 9a-d.** Same as fig. 7a-d except for JJA

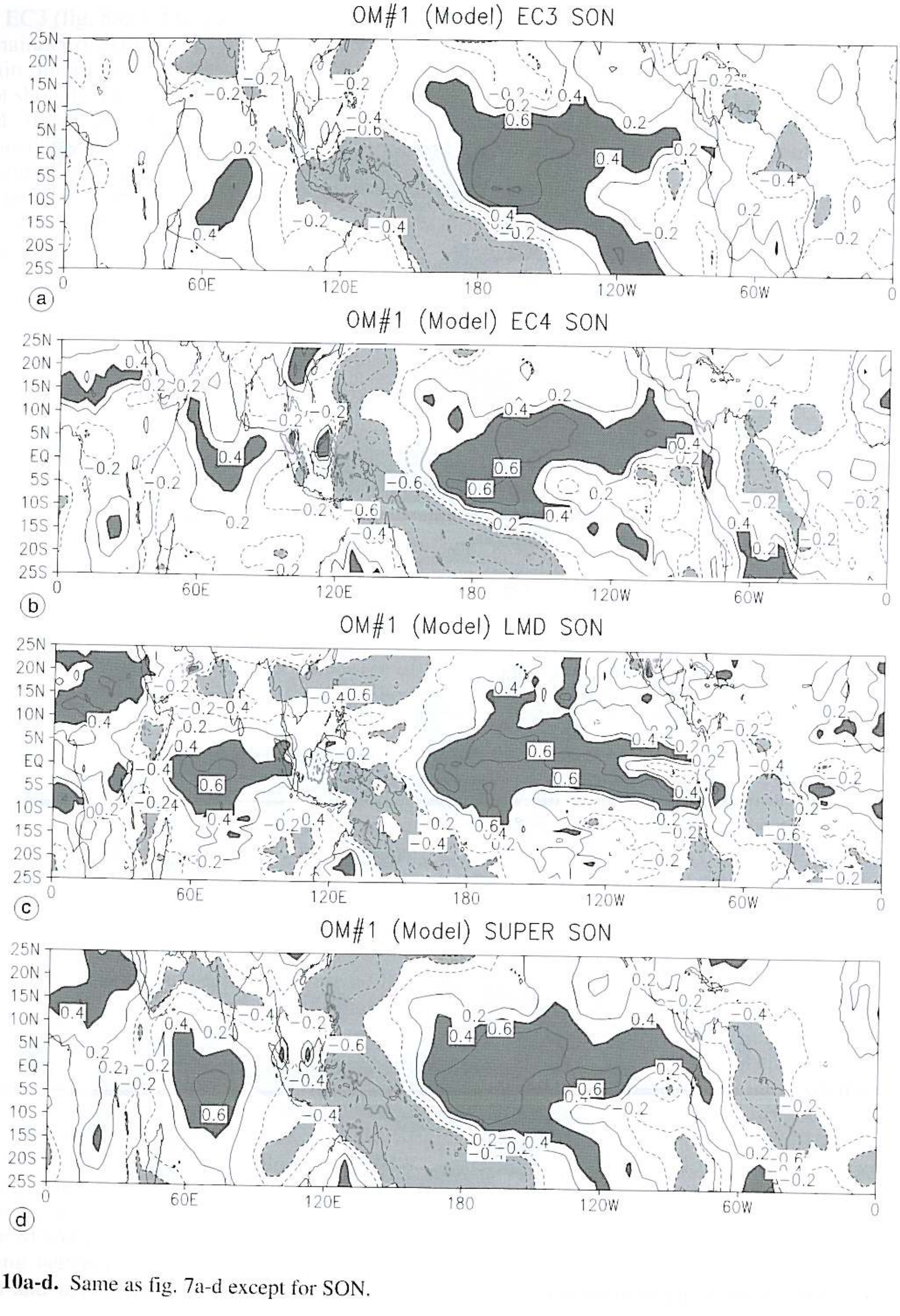


**Fig. 10a-d.** Same as fig. 7a-d except for SON.

in-phase rainfall anomalies between the Central Pacific and eastern equatorial Africa and Sri Lanka. These anomalies accompany the in phase SST variability between these regions, that is, a particularly warmer Western Indian Ocean in this season during EN years (*i.e* Moron *et al.*, 1998b).

Relative to JJA, the $OM_m$ patterns are more consistent between each other, with pattern correlations ranging from 0.54 (between EC3 and LMD) to 0.70 (between EC3 and EC4) (fig. 10d). The pattern correlations with the super-ensemble $OM_m$ are over 0.83. Compared to observations, the spatial behavior is rather similar to that of JJA (pattern correlations from 0.56 (EC4) to 0.68 (super-ensemble)), suggesting that these models do not alter their teleconnection structures sufficiently in response to changes in the background annual cycle (fig. 10a-d). There is a clear zonal out-of-phase between the Central Pacific on the one hand and the Western Pacific and the maritime continent on the other hand (fig. 10a-d). There are also positive correlations over the Western Indian Ocean. However, these positive correlations do not extend sufficiently west into East Africa, such that all models are not skilful in reproducing the in-phase behavior between the Central Pacific and East Africa. As for JJA, all models specifiy in-phase relationship between the Central Pacific and the Sahelian area, which is wrong if we consider observations (see fig. 6d, the result is dominated by September, since much less rain falls in October and November in the Sahel). The negative correlations observed over the whole of tropical America, and positive correlations over subtropical edges (La Plata, Caribbean Islands) are present for all models and quite consistent with the observations. The correlations with SST reveal almost the same features as JJA, except for the stronger in phase variability between the Central Pacific and Western Indian Ocean (not shown).

## 6. Conclusions

The response of three different AGCMs (EC4 at T30 resolution; EC3 at T21 resolution; LMD at 96×72 grid-points resolution) to prescribed SST over the period 1961-1993 has been studied, focusing on tropical circulation. Three runs of each model have been made, only differing by their initial conditions. The SST-forced components amongst the runs of one model and amongst all the runs has been analysed for various indices (SOI, regional rainfall indices, wind-shear monsoon index). The most skilful and the most reproducible modes of tropical rainfall have been extracted through multivariate analyses (SVD) as in Ward and Navarra (1997), MNRW98, Feddersen *et al.* (1999) and Moron *et al.* (2001a).

The mean annual cycle in the tropics was first compared amongst the models and with observations. The main problems in these models are the weakness of the Atlantic ITCZ in boreal winter (especially of EC4) and the displacement and intensity of highest rainfall in SE Asia in boreal summer. The highest rainfall totals are displaced southward from the equatorial Indian Ocean to the tropical Northwestern Pacific for EC3 and EC4, relative to observations. These and other errors can be expected to contribute to the discrepancies between model and observed teleconnection responses to SST, as identified in Sections 4 and 5 of the paper.

The model response to SST was first analysed using well-known large-scale tropical indices (SOI, wind-shear monsoon index and three regional rainfall indices of the Sahel, India and Nordeste). The performance of these models is quite consistent with other studies (*e.g.*, Sperber and Palmer, 1996). We have here begun to assess issues concerning how to combine the predictions from the different runs. For the regional indices, our optimum combination of the super-ensemble, as estimated using cross-validated multiple regression, yields more skill than any of the individual models (Krihsnamurti *et al.*, 2000). However, the super-ensemble contains a contribution from more runs, and it is possible that the increase in skill is merely attributable to an increased ensemble size, increasing the signal to noise ratio. To try and remove this effect, the skill of indices generated by combining one run from each of the three models was assessed. The mean skill of these indices was usually greater than the mean skill of the three individual models, providing evidence that the combination of models is adding some extra skill

(Krishnamurti *et al.*, 2000). The situation is less clear for the monsoonal wind-shear indices of West Africa and the tropical rainfall indices of India and the Sahel. For these generally lower skill indices, the skill of each model is very different. The optimum way to generate a prediction may be to give zero weight to the lowest skill models, but even if this is the case, the results suggest the need for a number of operational models, since all these models are superior for at least one of the indices studied. In other words, each model has its own strengths which allow it to contribute to the forecast of certain indices, even if it is rejected for other indices. For the low skill indices, it appears that some years are correctly specified by almost the whole set of runs, suggesting an inter-annual variability of skill-reproducibility, that provides an avenue for more detailed investigation.

As found in MNWR98 for one model, the leading patterns of the most skilful model modes are almost identical to the model modes maximising reproducibility amongst the runs. The global-scale features of the leading $OM_0$ modes are very similar between models, and largely describe the observed ENSO signal in each season. However, the $OM_m$ modes do have considerable differences between models. The differences in the $OM_m$ modes define the different ways in which each model responds to ENSO forcing. Thus, the model differences, such as the different parametrization schemes and resolution, give rise to different teleconnection structures. The differences are least in the tropical Pacific where there is strong local SST forcing, but even here, substantial differences amongst the model responses can be found. In particular, there is a strong meridional rainfall dipole over the Pacific in DJF and MAM for both EC4 and LMD models, whereas the dipole remains zonal for all seasons in the EC3 model.

Another major issue is the extension throughout the tropics of the anomalies associated with the ENSO-LNSO events. The leading mode is generally characterised by an out-of-phase pattern between the central and eastern equatorial Pacific and equatorial Indian Ocean on the one hand and almost the remaining tropical belt on the other hand with largest weights often over the SPCZ area, the northwestern tropical Pacific around Micronesia and Northern South America. However, considerable differences are found by season, as we have quantified by calculating pattern correlations between the patterns for consecutive seasons. For example, in observations, there is a very strong contrast in the observed mode pattern from MAM to JJA, and from JJA to SON. The models also displayed strong evolution season-by-season of the leading teleconnection structure. One general deficiency was that the models' SON teleconnection mode was rather too similar to the JJA mode. If we consider the total variance explained by the OM modes, the influence of ENSO-LNSO events in the models is strongest in DJF and SON and weakest in MAM and JJA. The weak results for JJA may represent problems with the models' ability to correctly capture the JJA teleconnections during the boreal summer monsoon season. The known observed teleconnections during ENSO that generally lead to negative rainfall anomalies over Southern Africa (DJF) and positive ones over equatorial East Africa (SON) are not really simulated by any of the models. Likewise, for the Sahelian belt, which experiences negative anomalies in JJA during ENSO (especially since 1970) actually experiences positive anomalies in EC4 and LMD, and near zero anomalies in EC3. It is possible in all cases that the models displace the real teleconnections, creating anomalies over the Western Indian Ocean (instead of Southern Africa in DJF), Central Indian Ocean (instead of equatorial East Africa in SON) and the Gulf of Guinea area (instead of the Sahel in JJA). The exact location of the displacement is model specific, as revealed by the relatively low pattern correlations between each of the model's $OM_m$ pattern. Thus the results endorse the combination of the models taking account of each model's spatial teleconnection structures, such as could be done with a super-ensemble extended SVDA or CCA approach. Indeed, we have confirmed here that the leading base patterns identified by the individual OM analyses will indeed be almost identical (pattern correlations of about 0.98) to super ensemble extended base patterns that can be used as the basis for a combination of the models. This should represent a further advance beyond the combination of indices using multiple regression.

## Acknowledgements

The rainfall data set used in this study was kindly provided by Mike Hulme (CRU, Norwich). The runs were conducted under EC contract DICE-EV5V-CT94-0538 and the stay of one of us (VM) at IMGA was partially supported by this EC contract. Discussions with K. Miyakoda were also fruitful during the development of this work.

*REFERENCES*

BALSAMEDA, M.A., M.K. DAVEY and D.L.T. ANDERSON (1994): Seasonal dependence of ENSO prediction skill, Hadley Centre for Climate Prediction and Research, *Report* n. 51.

BARNETT, T.P. (1995): Monte-Carlo forecasting, *J. Climate*, **8**, 1005-1021.

BARNETT, T.P., K. ARPE, L.JI.M. BENGTSSON and A. KUMAR (1997): Potential predictability and AMIP implications of midlatitude climate variability in two general circulation models, *J. Climate*, **10**, 2321-2329.

BELTRANDO, G. (1990): Space-time variability of rainfall in April and October-November over East-Africa during 1932-1983, *Int. J. Climatol.*, **10**, 679-690.

BELTRANDO, G. and P. CAMBERLIN (1993): Inter-annual variability of rainfall in the eastern horn of Africa and indicators of atmospheric circulation, *Int. J. Climatol.*, **13**, 533-546.

BENGTSSON, L., K. ARPE, E. ROECKNER and U. SCHULZWEIDA (1996): Climate predictability experiments with a general circulation model, *Climate Dyn.*, **12**, 261-278.

BRETHERTON, C.S., C. SMITH and J.M. WALLACE (1992): An intercomparison of methods for finding coupled patterns in climate data, *J. Climate*, **5**, 541-560.

DAÏ, A., Y.I. FUNG and A.D. DEL GENIO (1997): Surface observed global land precipitation variations during 1900-1988, *J. Climate*, **10**, 2943-2962.

DAVIES, J.R., D.P. ROWELL and C.K. FOLLAND (1997): North Atlantic and European seasonal predictability using an ensemble of multi-decadal AGCM simulations, *Int. J. Climatol.*, **17**, 1263-1280.

FEDDERSEN, H., A. NAVARRA and M.N. WARD (1999): A statistical correction approach for dynamical seasonal prediction, *J. Climate*, **12**, 1974-1989.

FONTAINE, B. and S. JANICOT (1992): Wind field coherence and its variations over West-Africa, *J. Climate*, **5**, 512-524.

FONTAINE, B., S. JANICOT and V. MORON (1995): Rainfall anomaly patterns and wind field signals over West-Africa in August (1958-1989), *J. Climate*, **8**, 1503-1510.

GADGIL, S. and S. SAJANI (1998): Monsoon precipitation in the AMIP runs, *Climate Dyn.*, **14**, 659-689.

GRAHAM, N.E., T.P. BARNETT, R. WILDE, M. PONATER and S. SCHUBERT (1994): On the roles of tropical and midlatitude SSTs in forcing inter-annual to interdecadal variability in the winter Northern Hemisphere circulation, *J. Climate*, **7**, 1416-1440.

HALPERT, M.S. and C.F. ROPELEWSKI (1992): Surface temperature patterns associated with the Southern Oscillation, *J. Climate*, **5**, 577-593.

HARZALLAH, A. and R. SADOURNY (1995): Internal *versus* SST-forced atmospheric variability as simulated by an atmospheric general circulation model, *J. Climate*, **8**, 474-495.

HENSE, A. and U. ROEMER (1995): Statistical analysis of tropical climate anomaly simulations, *Climate Dyn.*, **11**, 178-152.

HULME, M. (1991): An intercomparison of model and observed global precipitation climatologies, *Geophys. Res. Lett.*, **18**, 1715-1718.

KANG, I.S. and N.C. LAU (1986): Principal modes of atmospheric variability in model atmospheres with and without anomalous SST forcing in the tropical Pacific, *J. Atmos. Sci.*, **43**, 2719-2735.

KRISHNAMURTI, T.N., C.M. KISHTAWAL, Z. ZHANG, T. LAROW, D. BACHIOCHI, E. WILLIFORD, S. GADGIL and S. SURENDRAN (2000): Multimodel ensemble forecasts for weather and seasonal climate, *J. Climate*, **13**, 4196-4216.

KUMAR, A. and M.P. HOERLING (1995): Prospects and limitations of seasonal atmospheric GCM predictions, *Bull. Am. Meteorol. Soc.*, **74**, 335-345.

KUMAR, A. and M.P. HOERLING (1998): Annual cycle of Pacific North American seasonal predictability associated with different phases of ENSO, *J. Climate*, **11**, 3295-3308.

LATIF, M., J. BIERCAMP, H. VON STORCH, M. MCPHADEN and E. KIRK (1990): Analyses of tropical anomalies simulated by an AGCM, *J. Climate*, **3**, 509-521.

LAU, N.C. (1985): Modeling the seasonal dependence of the atmospheric response to observed El Niño in 1962-1976, *Mon. Weather Rev.*, **113**, 1970-1996.

LAU, N.C. and M.J. NATH (1994): A modeling study of the relative roles of tropical and extratropical SST anomalies in the variability of the global atmosphere-ocean system, *J. Climate*, **7**, 1184-1207.

LAU, K.M. and S. YANG (1996): The asian monsoon and predictability of the tropical ocean-atmosphere system, *Q. J. Meteorol. Soc.*, **122**, 945-967.

LI, Z.X. (1999): Ensemble atmospheric GCM simulation of climate variability from 1979 to 1994, *J. Climate*, **12**, 986-1001.

LIANG, X.Z., K.R. SPERBER, W.C. WANG and A.N. SAMEL (1997): Predictability of SST forced climate signals in two atmospheric general circulation models, *Climate Dyn.*, **13**, 391-415.

LIVEZEY, R.E. and T.M. SMITH (1999): Covariability of aspects of North American Climate with global seas surface temperatures on inter-annual to interdecadal timescales, *J. Climate*, **12**, 289-302.

MIYAKODA, K., N. WARD and A. NAVARRA (1999): Tropical-wide teleconnection and oscillation: part II, the ENSO-monsoon system, *Q. J. Meteorol. Soc.*, **125**, 2937-2964.

MONTROY, D.L. (1997): Linear relation of Central and Eastern North American precipitation to tropical Pacific SST anomalies, *J. Climate*, **10**, 541-558

MORON, V. (1994): Guinean and sahelian rainfall indices at monthly and seasonal scale (1933-1990), *Int. J. Climatol.*, **14**, 325-341.

MORON, V., A. NAVARRA, M.N. WARD and E. ROECKNER (1998a): Skill and reproducibility of seasonal rainfall patterns in the tropics in ECHAM4 GCM simulations with prescribed SST, *Climate Dyn.*, **14**, 83-100.

MORON, V., R. VAUTARD and M. GHIL (1998b): Trend, decadal and inter-annual variability of global SST, *Climate Dyn.*, **14**, 545-569.

MORON, V., M.N. WARD and A. NAVARRA (2001a): Observed and SST-forced seasonal rainfall variability across tropical America, *Int. J. Climatol.* (in press).

MORON, V., A. NAVARRA, M.N. WARD, C.K. FOLLAND, P. FRIEDERICHS, K. MAYNARD and J. POLCHER (2001b): Analysing and combining atmospheric general circulation model simulations forced by prescribed SST: northern extratropical response, *Ann. Geofis.*, **44** (4), 781-794 (this volume).

NAVARRA, A., M.N. WARD and K. MIYAKODA (1999): Tropical-wide teleconnection and oscillation. Part I: teleconnections indices and type I/II states, *Q. J. Meteorol. Soc.*, **125**, 2909-2935.

OGALLO, L.J. (1988): Relationships between seasonal rainfall variability in East Africa and the southern oscillation, *J. Climatol.*, **8**, 33-44.

PALMER, T.N. (1986): The influence of the Atlantic, Pacific and Indian oceans on Sahel rainfall, *Nature*, **322**, 251-253.

PARKER, D.E., P.D. JONES, C.K. FOLLAND and A. BEVAN (1994): Interdecadal changes of surface temperature since the late nineteenth century, *J. Geophys. Res.*, **99**, 14373-14399.

POTTS, J.M., C.K. FOLLAND, I.T. JOLLIFFE and D. SEXTON (1996): Revised 'LEPS' scores for assessing climate model simulations and long-range forecasts, *J. Climate*, **9**, 34-53.

RAYNER, N.A., E.B. HORTON, D.E. PARKER, C.K. FOLLAND and R.B. HACKETT (1996): Version 2.2 of the global sea-ice and sea surface temperature data set 1903-1994, Hadley Centre for Climate Research, *Technical Note* n. 74.

RENSHAW, A.C., D.P. ROWELL and C.K. FOLLAND (1998): ENSO responses and low frequency weather variability in the North Pacific/American sector 1949-1993, *J. Climate*, **11**, 1073-1093.

ROECKNER, E., K. ARPE, L. BENGTSSON, M. CHRISTOPH, M. CLAUSSEN, L. DUMENIL, M. ESCH, M. GIORGETTA, U. SCHLESE and U. SCHULZWEIDA (1996): The atmospheric general circulation model ECHAM-4 model description and simulation of the present day climate, *Report* n. 218, MPI, Hamburg.

ROPELEWSKI, C.F. and M.S. HALPERT (1987): Global and regional scale precipitation and temperature patterns associated with El Niño/Southern Oscillation, *Mon. Weather Rev.*, **115**, 1606-1626.

ROPELEWSKI, C.F. and M.S. HALPERT (1996): Quantifying Southern Oscillation - precipitation relationships, *J. Climate*, **9**, 1043-1059.

ROWELL, D.P. (1998): Using an ensemble of multi-decadal GCM simulations to assess potential seasonal predictability, *J. Climate*, **11**, 109-120.

ROWELL, D.P., C.K. FOLLAND, K. MASKELL and M.N. WARD (1995): Variability of the summer rainfall over tropical summer rainfall over tropical North Africa (1906-1992): observations and modelling, *Q. J. Meteorol. Soc.*, **121**, 669-704.

SADOURNY, R. and K. LAVAL (1984): January and July performance of the LMD general circulation model, in *New Perspective in Climate Modelling*, edited by A. BERGER and C. NICOLIS (Elsevier), 173-198.

SERVAIN, J. (1991): Simple climatic indices for the tropical Atlantic ocean, *J. Geophys. Res.*, **96**, 137-146.

SMITH, T.M. and R.E. LIVEZEY (1999): GCM systematic errors correction and specification of the seasonal mean Pacific - North America region atmosphere from global SSTs, *J. Climate*, **12**, 273-288.

SPERBER, K.R. and T.N. PALMER (1996): Inter-annual tropical rainfall variability in general circulation models simulations associated with the atmospheric model intercomparison project, *J. Climate*, **9**, 2727-2750.

SRINIVASAN, G., M. HULME and C.G. JONES (1995): An evaluation of the spatial and inter-annual variability of tropical precipitation as simulated by GCMs, *Geophys. Res. Lett.*, **22**, 1697-1700.

STERN, W. and K. MIYAKODA (1995): Feasibility of seasonal forecasts inferred from multiple GCM simulations, *J. Climate*, **8**, 1071-1085.

WAGNER, R.G. and A.M. DA SILVA (1994): Surface conditions associated with anomalous rainfall in the guinea coastal region, *Int. J. Climatol.*, **14**, 179-208.

WARD, M.N. and A. NAVARRA (1997): Pattern analysis of ensemble GCM simulations with prescribed SST: boreal summer examples over Europe and the tropical Pacific, *J. Climate*, **10**, 2210-2220.

WEBSTER, P.J. and S. YANG (1992): Monsoon and ENSO: selectively interactive systems, *Q. J. Meteorol. Soc.*, **118**, 877-926.

XIE, P. and P.A. ARKIN (1996): Analyses of global monthly precipitation using gauge observations, satellites estimates and numerical model prediction, *J. Climate*, **9**, 840-858.

ZWIERS, F.W. (1996): Inter-annual variability and predictability in an ensemble of AMIP climate simulations conduced with the CCC GCM2, *Climate Dyn.*, **12**, 825-848.

ZWIERS, F.W. and V.V. KHARIN (1998): Intercomparison of inter-annual variability and potential predictability: an AMIP diagnostic subproject, *Climate Dyn.*, **14**, 517-528.

(received May 15, 2001;
accepted August 30, 2001)